Article

Simulations and Modeling of Intermediate Luminosity Optical Transients and Supernova Impostors

Amit Kashi [1] *

[1] Department of Physics, Ariel University, Ariel, POB 3, 40700, Israel

* Correspondence: kashi@ariel.ac.il ; Tel.: +972-3-914-3046 ; http://www.ariel.ac.il/sites/amitkashi

Version June 25, 2018 submitted to

Abstract: Intermediate-luminosity-optical-transients (ILOTs) are stellar outbursts with luminosity between those of classical novae and supernovae. They are divided into a number of sub-groups depending on the erupting progenitor and the properties of the eruption. Many of the ILOTs sit on the slanted Optical Transient Stripe (OTS) in the Energy-Time Diagram (ETD) that shows their total energy vs. duration of their eruption. We describe the different kinds of ILOTs that populate the OTS and other parts of the ETD. We also stand on similarities between Planetary Nebulae (PN) to ILOTs, and suggest that some PNe were formed in an ILOT event. The high energy part of the OTS is reserved to the supernova impostors – giant eruption of very massive stars. We show results of 3D hydrodynamical simulations of supernova impostors that expose the mechanism behind these giant eruptions, and present new models for recent ILOTs. We stand on the connection between different kinds of ILOTs, and suggest that they are powered by a similar source of energy – gravitational energy released by mass transfer.

Keywords: stellar evolution; late stage stellar evolution; binarity, transients, planetary nebulae

1. Introduction

Intermediate luminosity optical transients (ILOTs) are exotic transients which lies in between the luminosities of novae and supernovae (SN). The group consists of many different astronomical eruptions that at first appear to look different from one another, but found to have shared properties. The different types of ILOTs are described in section 2. The ILOTs we discuss in this paper and many more are classified according to their total energy and eruption timescale (see section 3) using a tool named the energy-time diagram (ETD; see http://phsites.technion.ac.il/soker/ilot-club/). Most ILOTs reside on the optical transient stripe (OTS) on the ETD, that gives us information about the power involved in the eruption and its magnitude. A recent version of the ETD can be found in [14] and in [24] published in the present special issue.

2. Types of ILOTs

The literature in recent years has been far from consistent in referring to transient events. Since many ILOTs are being discovered, time has arrived for everyone to converge on one naming scheme that will eliminate any ambiguity. In [12] we picked up the gauntlet and suggested a complete set of names for the new types of transients. Since then, there have been developments in the field and new types have been suggested. We therefore hereby update the classification scheme of ILOTs.

A. Type I ILOTs. Type I ILOTs is the term for the combined three groups listed below: ILRT, LRN and LBV giant eruptions. These events share many common physical processes, in particular being powered by gravitational energy released in a high-accretion rate event, according to the high-accretion-powered ILOT (HAPI) model, discussed below. The condition for an ILOT to be classified as type I is that the observing direction is such that the ILOT is not obscured from the observer by an optically thick medium.

1. **ILRT: Intermediate-Luminous Red Transients**. Events involving evolved stars, such as Asymptotic Giant Branch (AGB) stars and Extreme Asymptotic Giant Branch (ExAGB) stars, and similar objects, e.g., Red Giant Branch (RGB) stars. The scenario which leads to theses events is most probably a companion which accretes mass and the gravitational energy of the accreted mass supplies the energy of the eruption. Examples include NGC 300 OT, SN 2008S, M31LRN 2015 (note the self-contradiction in the names of the last two transients).
2. **LBV giant eruptions and SN Impostors**. Giant eruptions of Luminous Blue Variables (LBVs). Note that conventional S Dor eruptions are not included. These eruptions are the most energetic ones among ILOTs, and the energy released in one or a sequence of those eruptions can reach 10^{49} erg and possibly more. Examples include the 1837–1856 Great Eruption of η Car, the pre-explosion eruptions of SN 2009ip. ILRTs are the low mass relatives of LBV giant eruptions.
3. **LRN or RT: Luminous Red Novae or Red Transients or Merger-bursts.** These are powered by a full merger of two stars. The process of destruction of the less dense star onto the denser star releases gravitational energy that powers the transient. Examples include V838 Mon and V1309 Sco.

B. Type II ILOTs. Type II ILOTs is the name of a new type of binary-powered ILOTs [13]. The event may be similar to Type I ILOTs (type I), but different in the orientation of the observer, whose line of sight crosses a thick dust torus or shell that obscures a direct view of the binary system or the photosphere of the merger product.

The scenario for a type I ILOT is based on a strong binary interaction. Such an interaction can be a periastron passage similar to the Great Eruption of η Carinae [11], or a terminal merger. The interaction leads to an axisymmetrical mass ejection with a large departure from spherical symmetry, much like the morphologies of many planetary nebulae (e.g., [2,4,15,18,23]).

The obscuring matter would be in most cases equatorial, and will contain most of the ejected mass. Until this dust disperses the binary system will be obscured to the eyes of the observer in the visible and IR bands. The type II ILOT is accompanied by some polar mass ejection that may also forms dust. The polar dust and gas reprocess the radiation from the central source, hence allowing the observation of the type II ILOT, which becomes much fainter. A possible example is the outburst observed from the red supergiant N6946-BH1 in 2009 [1].

C. Proposed scenarios for ILOTs. Other types of ILOTs have been suggested to exist, and populate empty regions of the ETD.

1. **Mergerburst between a planet and a brown dwarf (BD)**. In this process [3] the planet is shredded into a disk, and the accretion lead to an outburst. The destruction of a component in a binary system and transforming it to an accretion disk is an extreme case of mass transfer processes in binary systems. The destruction of the planet before it hits the BD occurs because its average density is lower than that of the BD. In that scenario it is required that the planet enters the tidal radius. It may occur in a highly eccentric orbit that is perturbed. Once the planet is destructed, the remnant of the merger behaves similarly to other ILOTs, such as V838 Mon, but on a shorter time scale and with less energy. This process is a super Eddington process and these events occupy the lower part of the OTS on the ETD.
2. **Weak Outburst of a young stellar object (YSO).** In [14] it was suggested that the unusual outburst of the YSO ASASSN-15qi is an ILOT event, similar in many respects to V838 Mon, but much fainter and of lower total energy. The erupting system was young, but unlike the LRN, the secondary object that was tidally destroyed onto the primary main-sequence (MS) star was suggested to be a Saturn-like planet rather than another low mass MS star. Such ILOTs are unusual in the sense that they have low power and reside below the OTS.
3. **ILOT which created a Planetary Nebulae (PN).** In [25] we identified some intriguing similarities between PNe and ILOTs: (a) a linear velocity-distance relation, (b) bipolar structure, (c), expansion velocity of few $\times$100km s^{-1}, (d) total kinetic energy of $\approx 10^{46}$–10^{49} erg. We therefore suggest

that some PNe may have formed in an ILOT event lasting a few months (a short "lobe-forming" event). The power source is similar, namely, mass accretion onto a MS companion from the AGB (or ExAGB). Examples include the PN NGC 6302, and the pre-PNe OH231.8+4.2, M1-92, and IRAS 22036+5306.

3. Common properties of ILOTs

In [10] we noticed that when scaling the time axis for ILOTs of the three kinds, an amazing similarity in the light curve surfaces. From the peak or peaks of the lightcuve, the decline in the optical bands with time is similar for almost four magnitudes. This could not be a coincidence, and a common physical mechanism must have been involved in all ILOTs; one that resulted in a similar decline.

The high-accretion-powered ILOT (HAPI) model is a model that aims to focus on the shared properties of many of the ILOTs. In its present state, the model accounts for the source and the amount of energy involved in the events and for their timescales. The step of obtaining the exact decline rates of the events has not yet been performed, and is currently under work.

The HAPI model is built on the premise that the luminosity of the ILOT comes from gravitational energy of accreted mass that partially channeled to radiation. The radiation is eventually emitted in the visible, possibly after scattering and/or absorption and re-emission.

To quantitatively obtain the power of the transients, we start by defining M_a and R_a as the mass and radius (respectively) of star 'a', which accretes the mass. Star 'b' is the one that supplies the mass to the accretion; it is possibly a destructed MS star, as in V838 Mon and V1309 Sco, or alternatively an evolved star in an unstable phase of evolution that loses a huge amount of mass, as in the giant eruptions of η Car. The average total gravitational power is obtained by multiplying the average accretion rate and the potential well of the accreting star

$$L_G = \frac{G M_a \dot{M}_a}{R_a}. \tag{1}$$

The accreted mass may form an accretion disk or a thick accretion belt around star 'a'. In the case of a merger event this belt consists of the destructed star. The accretion time should be longer than the viscosity time scale for the accreted mass to lose its angular momentum, so it can be actually accreted. The viscosity timescale is scaled according to

$$t_{\rm visc} \simeq \frac{R_a^2}{\nu} \simeq 73 \left(\frac{\alpha}{0.1}\right)^{-1} \left(\frac{H/R_a}{0.1}\right)^{-1} \left(\frac{C_s/v_\phi}{0.1}\right)^{-1} \left(\frac{R_a}{5\,R_\odot}\right)^{3/2} \left(\frac{M_a}{8\,M_\odot}\right)^{-1/2} \text{days}, \tag{2}$$

where H is the thickness of the disk, C_s is the sound speed, α is the disk viscosity parameter, $\nu = \alpha\, C_s H$ is the viscosity of the disk, and v_ϕ is the Keplerian velocity. We scale M_a and R_a in equation (2) according to the parameters of V838 Mon [28]. For these parameters, the ratio of viscosity to Keplerian timescale is $\chi \equiv t_{\rm visc}/t_K \simeq 160$.

The accreted mass is determined by the details of the binary interaction process, and varies for different objects. We scale it by $M_{\rm acc} = \eta_a M_a$. Based on the modeled systems (V838 Mon, V 1309 Sco, η Car) this mass fraction is $\eta_a \lesssim 0.1$ with a large variation. The value of $\eta_a \lesssim 0.1$ can be understood as follows. If the MS star collides with a star and tidally disrupts it, as in the model for V838 Mon [26,27], the destructed star is likely be less massive than the accretor $M_{\rm acc} < M_b \lesssim 0.3 M_a$. In another possible case an evolved star loses a huge amount of mass, but the accretor gains only a small fraction of the ejected mass, as in the great eruption of η Car.

The viscosity time scale gives an upper limit on the accretion rate

$$\dot{M}_a < \frac{\eta_a M_a}{t_{\rm visc}} \simeq 4 \left(\frac{\eta_a}{0.1}\right) \left(\frac{\alpha}{0.1}\right) \left(\frac{H/R_a}{0.1}\right) \left(\frac{C_s/v_\phi}{0.1}\right) \left(\frac{R_a}{5\,R_\odot}\right)^{-3/2} \left(\frac{M_a}{8\,M_\odot}\right)^{3/2} M_\odot {\rm yr}^{-1}. \tag{3}$$

The maximum gravitational power is therefore

$$L_G < L_{\rm max} = \frac{GM_a\dot{M}_a}{R_a} \simeq 7.7\times10^{41}\left(\frac{\eta_a}{0.1}\right)\left(\frac{\chi}{160}\right)^{-1}\left(\frac{R_a}{5\,R_\odot}\right)^{-5/2}\left(\frac{M_a}{8\,M_\odot}\right)^{5/2}{\rm erg\,s^{-1}}, \quad (4)$$

where we replaced the parameters of the viscosity time scale with the ratio of viscosity to Keplerian time χ.

The upper bound on the OTS in the ETD is determined by equation (4), and describes a supper-Eddington luminosity. The upper bound might be crossed if the accretion efficiency η is higher and/or the stellar parameters of the accreting star are different. For most of the ILOTs the accretion efficiency is lower, hence they are located below the upper limit line, giving rise to the relatively large width of the OTS. The uncertainty in η_a is large and may be even above unity, but only in extreme cases. Therefore, one does not expect to find objects above the upper limit frequently. We also note that the above estimate was performed with the expressions relevant for a thin disk and a thick disk may need different treatment. A more accurate treatment requires hydrodynamic simulations together with radiation transfer for obtaining the radiation emitted in each waveband.

4. Giant Eruptions in Very Massive Stars

As mentioned above, the most energetic ILOTs are the LBV giant eruptions. There is some controversy about the identification of the stars which undergo giant eruption with LBVs, so for safety we will refer to them as Very Massive Stars, or VMS.

In [9] we used the hydro code `FLASH` [7] to model the response of a massive star to a high mass loss episode. The hydro simulation started with the results of a run of a modified version of the 1D stellar evolution code `MESA` [19–22] in which we obtained a model of an evolved VMS. The `MESA` stellar model we obtained had properties similar to those of Eta Carinae, known for its giant eruptions in the 19th century. We simulated hydrodynamically a giant eruption with the FLASH code using two approaches: (1) Removing a layer from the star using energy from inner layers. (2) Extracting energy from the core to outer layers that causes a spontaneous mass loss.

We found that the star developed a strong wind, powered by pulsation in the inner parts of the star. The strong eruptive mass loss phase lasted for a few years, followed by centuries of continually weakening mass loss. Figure (1) shows the resulted mass loss rate with time after the initiation of the giant eruption. The three different lines indicate different simulations with a different amount of mass removed from the VMS.

After about two centuries the mass loss rate of the star declined quite dramatically. The explanation for this behavior is the change in the stellar structure as a response to the huge mass loss in the giant eruption we simulated and the two hundred years of high mass loss rate that followed. At a certain time the structure became such that the mechanism that accelerated the wind – non-adiabatic κ-mechanism pulsations induced near the iron-bump – stopped being efficient. At that point the mass loss rate decreased.

Observationally, the decline in mass loss rate we obtained was observed in η Car in the last two decades. Variations in spectral properties of the star, especially near periastron passage and across the spectroscopic event, taught us that this change-of-state has been happening [5,6,16]. However the reason was at first unknown, until the simulations in [9] revealed the physical mechanism and demonstrated its work.

In follow up simulations we were able to use super-high resolution to simulate a giant eruption in 2D and 3D, for the first time. The purpose of doing so is to be able to investigate multidimensional effects that cannot be completely or at all addressed otherwise: convection and mixing, rotation, turbulence, hydrodynamical instabilities, meridional currents, tides, and especially multi-dimensional pulsation. These effects are known to considerably influence the stellar properties, and therefore, we expect them to have a significant impact on how a VMS recovers from an eruption.

Preprints (www.preprints.org) | NOT PEER-REVIEWED | Posted: 25 June 2018 doi:10.20944/preprints201806.0378.v1

Peer-reviewed version available at Galaxies 2018, 6, 82; doi:10.3390/galaxies6030082

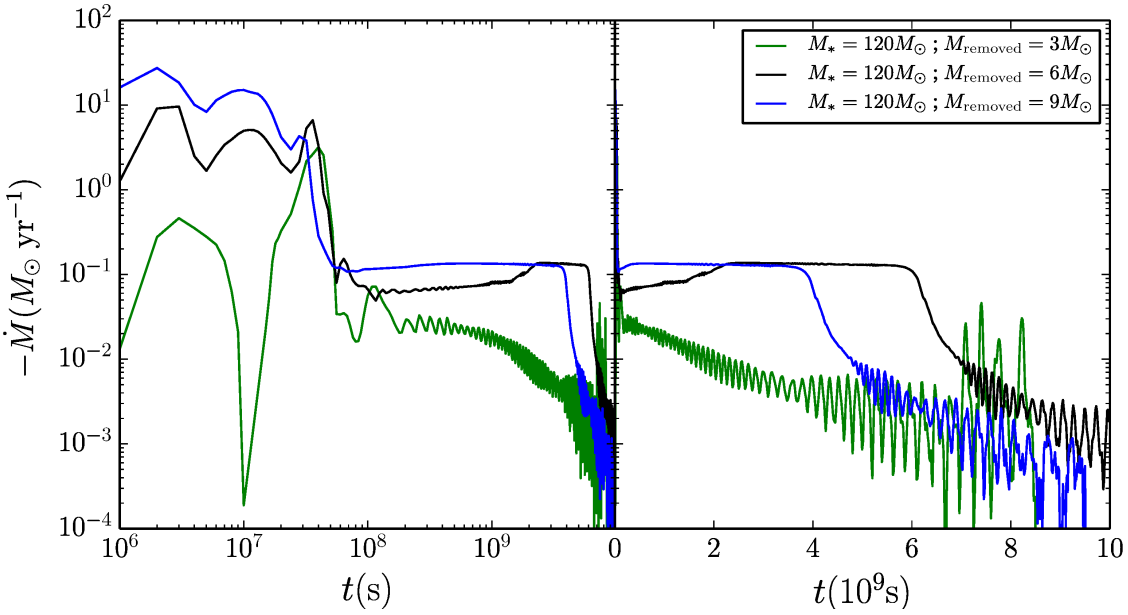

Figure 1. Mass-loss rate as a function of time for runs using the 120 $M_\odot$ VMS model and approach 1 for initiating a giant eruption. The three different lines indicate different simulations with a different amount of mass removed from the VMS. Two of the runs (the blue and black lines) show a change of state in the mass loss rate about $\approx$ 130 and $\approx$ 190 years (respectively) after the giant eruption started, respectively. By that the simulations reproduce the decline in mass loss observed in η Car in the last years, ($\sim$ 175 years after its great eruption), during which the mass loss rate has been declining by a factor of 2–4 (and possibly continues to decline).

Our 2D simulations produced an interesting result that could not have been obtained in 1D. Assuming that the source of the giant eruption is the core, the eruption caused a Richtmyer-Meshkov instability which propagated in the VMS during the days immediately following the giant eruption (Figure 2, left panel). That instability, in turn, caused strong dredging of species from the core to outer layers. Nuclear processed material from the core moved to the outer layers and eventually was ejected from the VMS. This may explain why the ejecta of η Car is nitrogen rich.

Figure 3 shows the stellar properties as a function of time after the giant eruption. In the 3D simulations, we found that the pulsations behaved much more chaotically and where much less coherent than in the 1D simulations. The 3 spatial degrees of freedom in the 3D simulation engender destructive interference of the pulsations (the chance of creating a constructive interference is low) that damp the waves before they reach the surface and eject mass. As a result, the mass-loss rate obtained after the eruption was smaller (Figure 1), and during the period spanning the first few years after the eruption the VMS reached an almost stable hydrostatic equilibrium.

In [11] we suggested that major LBV eruptions are triggered by binary interaction. The possible most problematic example to be considered against our claim was P Cygni, as it was believed to be a single star which underwent such an eruption. However [8] showed that even the eruption of P Cygni presented evidence of binary interaction, printed in the varying time gaps between its consequentive eruptions in the seventeenth century. Recently [17] used observations of P Cygni spanned over seven decades, along with signal processing methods to identify a periodicity in the stellar luminosity. The period they found is a possible indication for the presence of the companion suggested by [8] on the basis of the theoretical arguments. This strengthened the conjecture that probably all major LBV eruptions are triggered by interaction of a stellar companion.

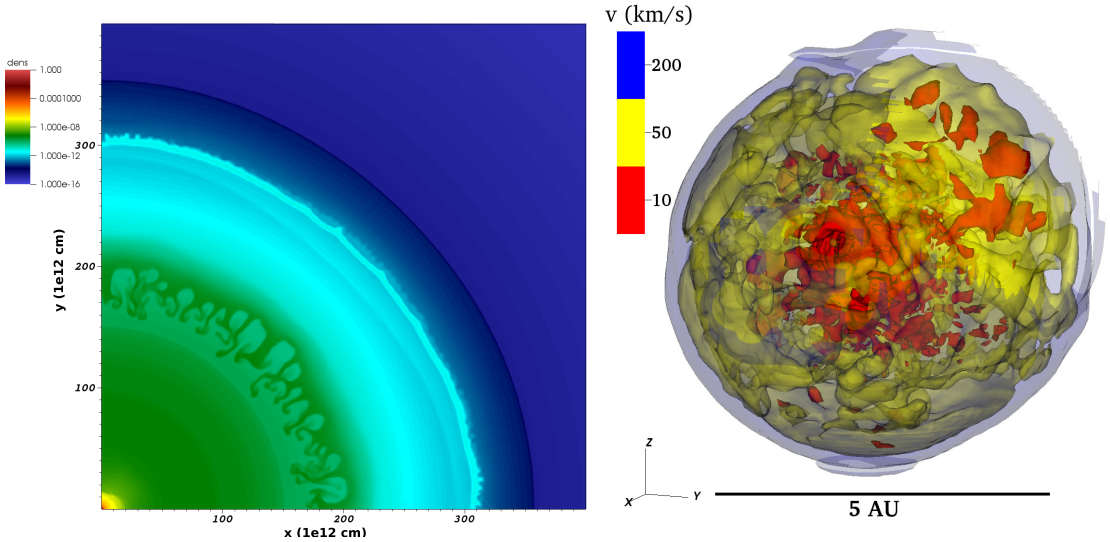

Figure 2. *Left:* A density map taken 5.8 days after the giant eruption. A layer experiencing the Richtmyer-Meshkov instability is seen at $r \simeq 1.6$–2.1×10^{14}cm. This causes strong mixing of elements from the core to outer layers, which explains why the ejecta of η Car is Nitrogen rich. Nuclear processed material from the core reaches the outer layers and is eventually ejected from the star. *Right:* Velocity 3D contours of the VMS and of the inner part of its clumpy wind 2.5 years after the giant eruption. The VMS has expended to $\approx 500 R_{\odot}$, and is highly convective. Parts in the star are moving inward as a result of pulsation, while the outer layers move outward and create wind. The resultant wind was found to be slower, and the mass-loss rate was found to be smaller then that suggested by observations and by our 1D model. The reason for this change is the incoherency of the pulsations in 3D.

5. Summary

We discussed different types of ILOTs and categorized them in a manner that makes order in the confused nomenclature in the field. We reviewed commonalities between these types and the HAPI model that suggest they are all gravitationally powered. We put the spot light on the most massive and energetic outburst that consist of the ILOTs group, the giant eruption in VMSs. The simulations we showed explain the mechanism being the strong mass loss after the giant eruptions, and account for the change of state in the mass loss more than 100 years after the eruption.

Acknowledgments: I thank Noam Soker and Amir Michaelis for helpful comments. Support from the the Authority for Research & Development in Ariel University and the Rector of Ariel University is gratefully acknowledged. This work used the Extreme Science and Engineering Discovery Environment (XSEDE) TACC/Stampede2 at the service-provider through allocation TG-AST150018. This work was supported by the Cy-Tera Project, which is co-funded by the European Regional Development Fund and the Republic of Cyprus through the Research Promotion Foundation.

Abbreviations

The following abbreviations are used in this manuscript:

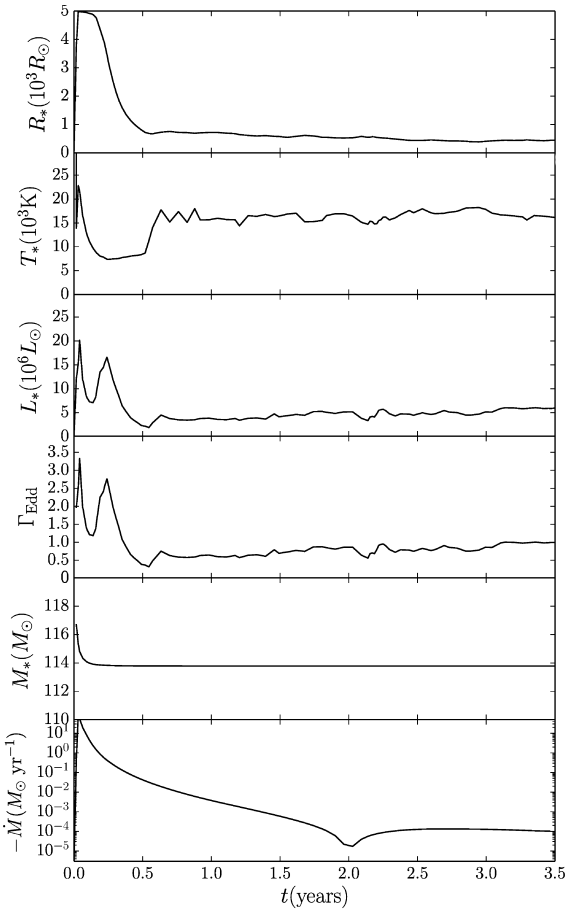

Figure 3. Results of one of our 3D simulations showing the recovery of a non-rotating VMS of 120 $M_\odot$ after removing an outer layer of 6 $M_\odot$ according to approach 2 (as a result of extracting energy from the core). From top to bottom, the panels show the stellar radius, effective temperature, luminosity, mass, Eddington ratio, and mass-loss rate. The temperature, radius and luminosity are calculated at optical depth $\tau = 3$. This figure can be compared to the right panel of figure 3 in [9], which shows the equivalent 1D simulation. In this 3D simulation, the first few years after the eruption bring the star to an almost stable hydrostatic equilibrium. The mass-loss rate is roughly two orders of magnitude smaller than that in the 1D simulation. Although the results of this preliminary work are still under study, they are probably due to the lower coherency of the pulsations in the 3D compared to the 1D simulation. The three spatial degrees of freedom engender destructive interference of the pulsations that damp the waves before they reach the surface and eject mass.

AGB	Asymptotic Giant Branch
ASASSN	All-Sky Automated Survey for Supernovae
BD	Brown Dwarf
ETD	Energy-Time Diagram
ExAGB	Extreme Asymptotic Giant Branch
HAPI	High Accretion Powered ILOT
ILOT	Intermediate Luminosity Optical Transient
ILRT	Intermediate Luminosity Red Transient
LBV	Luminous Blue Variable
LRN	Luminous Red Nova
MESA	Modules for Experiments in Stellar Astrophysics
MS	Main Sequence
OTS	Optical Transient Stripe
PN	Planetary Nebulae
SN	Supernova
VMS	Very Massive Star
YSO	Young Stellar Object

References

1. Adams, S. M., Kochanek, C. S., Gerke, J. R., Stanek, K. Z., & Dai, X. 2017, MNRAS, 468, 4968
2. Balick, B. 1987, AJ, 94, 671
3. Bear, E., Kashi, A., & Soker, N. 2011, MNRAS, 416, 1965
4. Corradi, R. L. M., & Schwarz, H. E. 1995, A & A, 293, 871
5. Davidson, K., Ishibashi, K., Martin, J. C., & Humphreys, R. M. 2018, ApJ, 858, 109
6. Davidson, K., Martin, J., Humphreys, R. M., et al. 2005, AJ, 129, 900
7. Fryxell, B., Olson, K., Ricker, P., et al. 2000, ApJS, 131, 273
8. Kashi, A. 2010, MNRAS, 405, 1924
9. Kashi, A., Davidson, K., & Humphreys, R. M. 2016, ApJ, 817, 66
10. Kashi, A., Frankowski, A., & Soker, N. 2010, ApJL, 709, L11
11. Kashi, A., & Soker, N. 2010, ApJ, 723, 602
12. Kashi, A., & Soker, N. 2016, Research in Astronomy and Astrophysics, 16, 99
13. Kashi, A., & Soker, N. 2017a, MNRAS, 467, 3299
14. Kashi, A., & Soker, N. 2017b, MNRAS, 468, 4938
15. Manchado, A., Guerrero, M. A., Stanghellini, L., & Serra-Ricart, M. 1996, The IAC morphological catalog of northern Galactic planetary nebulae (Publisher: La Laguna, Spain: Instituto de Astrofisica de Canarias (IAC)), 1996, Foreword by Stuart R. Pottasch, ISBN: 8492180609
16. Mehner, A., Davidson, K., Humphreys, R. M., et al. 2015, A & A, 578, A122
17. Michaelis, A. M., Kashi, A., & Kochiashvili, N. 2018, New Astronomy, 65, 29
18. Parker, Q. A., Bojičić, I. S., & Frew, D. J. 2016, Journal of Physics Conference Series, 728, 032008
19. Paxton, B., Bildsten, L., Dotter, A., et al. 2011, ApJS, 192, 3
20. Paxton, B., Cantiello, M., Arras, P., et al. 2013, ApJS, 208, 4
21. Paxton, B., Marchant, P., Schwab, J., et al. 2015, ApJS, 220, 15
22. Paxton, B., Schwab, J., Bauer, E. B., et al. 2018, ApJS, 234, 34
23. Sahai, R., Morris, M. R., & Villar, G. G. 2011, AJ, 141, 134
24. Soker, N. 2018, Galaxies, 6, 58
25. Soker, N., & Kashi, A. 2012, ApJ, 746, 100
26. Soker, N., & Tylenda, R. 2006, MNRAS, 373, 733
27. Tylenda, R., & Soker, N. 2006, A & A, 451, 223
28. Tylenda, R., Soker, N., & Szczerba, R. 2005, A & A, 441, 1099